Extended scaling factors for in situ cosmogenic nuclides: New measurements at low latitude

Darin Desilets [a,*], Marek Zreda [a], T. Prabu [b]

[a] *Department of Hydrology and Water Resources, University of Arizona, Tucson, AZ 85721, USA*
[b] *Raman Research Institute, Bangalore, 560 080, India*

Abstract

Production rates of cosmogenic nuclides at the earth's surface are controlled by the intensity of energetic cosmic-ray nucleons, which changes rapidly with elevation. An incomplete knowledge of how nucleon fluxes vary with elevation remains a major obstacle to utilizing cosmogenic nuclides as geochronometers in applications requiring highly accurate ages. One problem is that attenuation characteristics depend on nucleon energy. Measurements of high-energy (>50 MeV) nucleon fluxes tend to give shorter attenuation lengths than low-energy (<1 MeV) fluxes, but these differences are not well characterized due to a lack of data at lower energies. Another problem is that the atmospheric attenuation length for nucleon fluxes varies with the geomagnetic cutoff rigidity (a parameter related to geomagnetic latitude), R_C, and that there has been an incomplete mapping of nucleon fluxes at high R_C (low geomagnetic latitude). We report new measurements of nucleon fluxes from altitude transects in Hawaii ($R_C = 12.8$ GV) and Bangalore, India ($R_C = 17.3$ GV). Our measurements in Hawaii of low-energy neutrons (median energy 1 eV) and energetic nucleons (median energy 140 MeV) confirm that nucleon scaling functions are energy-dependent in the range of energies at which cosmogenic nuclides are produced. Our measurements in southern India extend our previously reported scaling model for spallation reactions [D. Desilets, M. Zreda, Spatial and temporal distribution of secondary cosmic-ray nucleon intensity and applications to in situ cosmogenic dating. Earth Planet. Sci. Lett. 206 (2003) 21–42] from $R_C = 13.3$ GV to $R_C = 17.3$ GV, nearly the highest cutoff rigidity on earth. The anomalously high cutoff rigidity over India provides a geomagnetic shielding condition that is effectively the same as would be observed at the geomagnetic equator in a dipole field with an intensity 1.2 times the modern value. This makes it possible to scale low-latitude production rates to paleomagnetic fields that are stronger than the present dipole field.
© 2006 Elsevier B.V. All rights reserved.

1. Introduction

The application of in situ cosmogenic nuclides to surface exposure dating requires accurate knowledge of how production rates vary in space and time. Nucleon interactions are responsible for most cosmogenic nuclide production in surface rocks at sea level and are by far the dominant production mechanism at high elevations [1]. Because nucleon fluxes are very sensitive to elevation, increasing by two orders of magnitude from sea level to the tropopause, small inaccuracies in

---

* Corresponding author. Tel.: +1 520 621 4072.
  E-mail address: ddesilet@hwr.arizona.edu (D. Desilets).

nucleon scaling parameters can lead to large uncertainties in determining production rates when these errors are propagated over a large elevation range.

Cosmic-ray nucleon fluxes at the earth's surface are generated in particle cascades that are initiated at the top of the atmosphere by energetic protons and heavier nuclei of the galactic cosmic-ray flux [2]. In the troposphere, secondary cosmic-ray nucleon fluxes diminish with increasing atmospheric depth according to:

$$J_2 = J_1 \exp\left(\frac{x_1 - x_2}{\Lambda}\right) \qquad (1)$$

where J_1 and J_2 are the nucleon fluxes at depths x_1 and x_2 (g cm^{-2}) and Λ (g cm^{-2}) is the nucleon attenuation length.

It has long been established that the value of Λ depends on cutoff rigidity and altitude [3]. Recently, Desilets and Zreda [4,5] pointed out that Λ at a particular location may also be a function of median nucleon energy and that this dependence could explain inconsistencies between scaling models derived from instruments having different energy sensitivities.

Because cosmogenic nuclides are produced at widely different median energies, scaling factors should be nuclide-dependent. However, as an approximation [5] assumed that because median energies for most spallation reactions relevant to terrestrial cosmogenic dating (60–140 MeV) are sufficiently close to the median energy of the neutron monitor (140 MeV), neutron monitor measurements can be used to scale all spallation reactions. That approximation is necessary because precise experimental data on how the nucleon energy spectrum changes with atmospheric depth are lacking in the 60–140 MeV range. Most of the data on how nucleon fluxes vary in space and time are from neutron monitor surveys and from airborne measurements of low-energy neutron fluxes. These two types of surveys measure widely separated energy bands that bracket the median energies at which all of the commonly used cosmogenic nuclides are produced.

This investigation has two main purposes. One is to verify that the energy dependence of nucleon scaling functions is important in the troposphere. We address this question by comparing recent measurements of nucleon fluxes in two energy bands: one corresponding to low-energy neutron activation reactions and the other corresponding to energetic spallation reactions. We expect based on [5]'s analysis of published cosmic-ray data that differences in scaling functions should be greatest at low latitude. Our measurements were motivated by a lack of low-energy (<1 MeV) neutron flux surveys below 5000-m altitude and the need to compare such data with more energetic fluxes measured by a neutron monitor. The second purpose of this work is to extend [5]'s scaling model for spallation reactions to lower geomagnetic latitude/higher geomagnetic field strength. That scaling model applies to cutoff rigidities (R_C) from 0 to 13.3 GV, the highest cutoff rigidity attained in [6]'s 1965 solar minimum cosmic-ray survey. In a dipole model of earth's present magnetic field, which in cosmogenic dating is often assumed for paleomagnetic fields for lack of better knowledge [7], R_C = 13.3 is equivalent to a geomagnetic latitude of 19°. Anomalously high cutoff rigidities over southern India created by non-dipole components of the geomagnetic field make it possible to extend those measurements to both lower geomagnetic dipole latitude and, equivalently, higher paleomagnetic field strength. In this work, we update our scaling model to incorporate measurements from southern India, which at R_C = 17.3 GV is close to the highest cutoff rigidity on earth.

2. Experimental

Altitude profiles of nucleon fluxes were obtained at two low-latitude locations: Hawaii and near Bangalore, India (Fig. 1). At these locations, it was possible to obtain ground-based measurements over a large elevation range at nearly constant R_C. In Hawaii, we measured high-energy nucleon fluxes from a car using a mobile neutron monitor and we measured low-energy neutron fluxes from a small airplane. In India, a neutron monitor identical to the one in Hawaii was used in a ground-based survey and later was transferred to an airplane for high-altitude measurements.

In this work, 'high-energy' and 'low-energy' are defined by the energy responses of our instruments. Although both instruments record a continuous distribution of energies, the median energy responses are substantially different (Fig. 2). The high-energy nucleon fluxes measured with the mobile neutron monitor correspond to a median nucleon energy of ∼140 MeV [9]. Low-energy neutron fluxes were measured using unshielded ^{3}He-filled proportional counters, which have a median energy response of ∼1 eV. The low-energy neutrons recorded by the unshielded proportional counters correspond closely to the energy band for neutron activation reactions. The high-energy nucleons recorded by the neutron monitor correspond approximately to the energy band for spallation reactions.
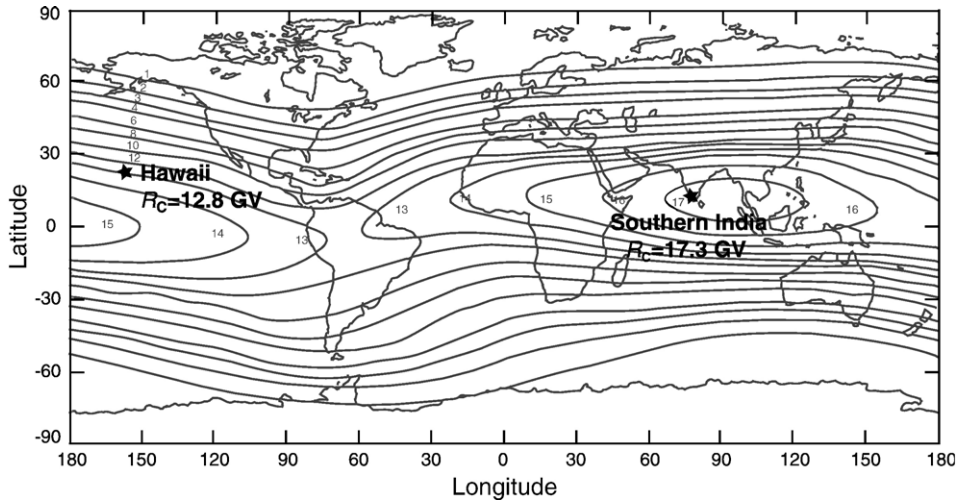
Fig. 1. Altitude survey locations. Contours show effective vertical cutoff rigidity (R_C) for 1980 [8].

2.1. High-energy nucleon fluxes in India and Hawaii

2.1.1. Mobile neutron monitor

A neutron monitor responds to energetic cosmic-ray nucleons indirectly through a complex series of interactions. In the first interaction, an energetic cosmic-ray nucleon (>50 MeV) excites a lead nucleus, which de-excites by emitting evaporation neutrons with energies in the 1–10 MeV range [9]. These fast neutrons are rapidly thermalized through elastic collisions in a layer of hydrogen-rich material (usually paraffin or polyethylene) that surrounds the lead on all sides. The hydrogenous material on the inside of the lead is referred to as the moderator and the material on the outside is known as the reflector. The reflector serves the dual purpose of moderating the neutrons generated in the lead and shielding the instrument from neutrons generated in outside materials [9]. This shielding is necessary because fluxes of low-energy neutrons from the external
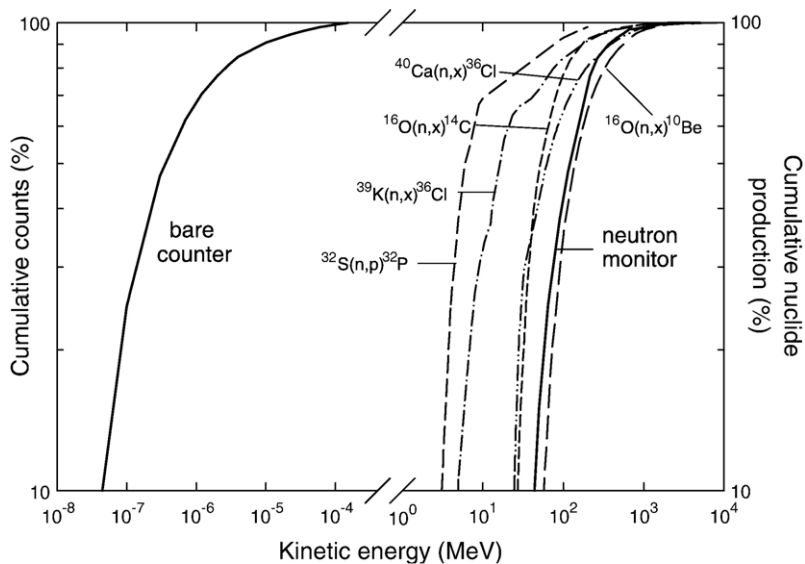

Fig. 2. Energy sensitivities for a bare neutron detector and an NM-64 neutron monitor compared with excitation functions for several commonly used cosmogenic nuclides [10]. Cumulative production from thermal neutron reactions (e.g. $^{35}Cl(n,\gamma)^{36}Cl$) would closely follow the cumulative response for the bare detector.

Table 1
Dimensions of the neutron monitor used in this work (AZ NM) and for two commonly used neutron monitors (NM64 and IGY)

	IGY	NM-64	Arizona NM
Counters			
Active length (cm)	86.4	191	33
Diameter (cm)	3.8	14.8	2.5
Pressure (atm)	0.6	0.3	10
Gas	BF_3	BF_3	^3He
Inner moderator thickness (cm)	3.2	2.0	2.5
Lead thickness (g cm)	13.5	13.8	10.2
Reflector thickness (cm)	28	7.5	18

environment depend on local conditions (e.g. soil moisture content, soil chemistry, proximity to high *Z* objects) that are highly variable between locations. At the center of the instrument are proportional counter tubes filled with a neutron-sensitive gas such as $^{10}BF_3$ or ^3He. A count is recorded when a thermal neutron is captured in the counter tube by the neutron-sensitive gas.

The primary advantage of the neutron monitor is that it yields a high count rate using a simple design that can be constructed from easily obtainable materials and equipment. However, a disadvantage in conventional neutron monitor designs (IGY and NM-64) is that massive amounts of lead are required (1600 kg per counter tube for NM-64 [9]), which presents a formidable logistical challenge in conducting neutron monitor surveys.

To gain greater mobility, we constructed a neutron monitor with substantially smaller dimensions (Table 1, Fig. 1 in the Appendix) than are specified for the IGY and NM-64 type instruments [9]. We used smaller detectors, which permitted a proportionate reduction in the required amounts of lead and paraffin. To compensate for the smaller sensitive volume of our detectors and the reduced amounts of lead, we used ^3He-filled tubes that are twice as sensitive per unit volume as the BF_3-filled detectors conventionally used in IGY an NM-64 neutron monitors. Previous experiments have shown that the respective use of smaller horizontal dimensions or ^3He instead of BF_3 in the counter tube has a negligible effect on the neutron monitor response [11,12]. Nonetheless, to check that the response of our instrument is similar to that of neutron monitors employed in the global neutron monitor network and in past sea-level latitude surveys, we performed measurements in Hawaii (R_C = 12.8 GV), to compare with extensive measurements conducted there previously [11]. Our results from Hawaii are described in Section 3.1.

An upper limit on the constant background count rate of our detectors was found by shielding a counter tube with a 0.7-mm-thick cadmium sleeve surrounded by 30 cm of paraffin. The shielded counter was placed in the basement of a three-story building to further reduce the contribution of neutrons generated by cosmic-rays. The resulting count rate of 0.062 ± 0.010 cpm ($\sim 1\%$ of the sea-level high-latitude count rate) is probably caused by trace amounts of alpha-emitting radionuclides in the aluminum counter walls [13,14]. This level of background is consistent with the background observed in NM-64 and IGY neutron monitors [13].

2.1.2. Land-based measurements

Altitude transects were obtained by transporting the neutron monitor by car from sea level to mountain sites. In April 2000, we measured neutron monitor count rates in Hawaii (R_C = 12.8 GV) along a transect from Kailua-Kona (sea level) to Mauna Kea (4205 m). In April 2002, we conducted a transect in India (R_C = 17.3 GV) along a route from Bangalore (949 m) to Calicut (sea level) and then to Doda Beta (2637 m). One detector malfunctioned in India and therefore only results from two of the three detectors are reported.

During the surveys in India and Hawaii temporal variations in secondary cosmic-ray intensity recorded by the Haleakala, Hawaii (R_C = 12.8 GV, 3030 m) neutron monitor were <2%. Corrections for temporal changes in cosmic-ray intensity were neglected because they do not change the value or uncertainty of attenuation lengths measured in India or Hawaii.

2.1.3. Airborne measurements

On May 8, 2002, we extended the altitude range of our survey at 17.3 GV by measuring neutron fluxes from the cabin of an aircraft provided by the Indian Air Force (data given in Table 1 in the Appendix). The airplane was kept at a uniform pressure–altitude for eight different altitudes. Below 3400 m, the airplane flew unpressurized and pressure was logged at 5-min intervals from a pressure sensor located inside of the cabin. Above 3400 m, the cabin was pressurized and we relied on manual recordings of the airplane's altimeter to determine the outside pressure. An airplane altimeter reads pressure from a sensor in the nose or wing and converts this pressure to altitude according to the ICAO International Standard Atmosphere model [15]. Pressures were calculated by converting the recorded altitudes back to units of atmospheric pressure using the ICAO International Standard Atmosphere model.

2.2. Low-energy neutron fluxes at Hawaii

2.2.1. Thermal neutron detector

Measurements of low-energy neutron fluxes were made from the tail compartment of a four-seat airplane. To obtain low-energy sensitivity we employed the same [3]He counter tubes and electronics modules used in the neutron monitor, but without lead or paraffin (Fig. 2 in the Appendix). The energy sensitivity of this instrument is controlled by the thermal neutron absorption cross section for [3]He, which has an energy dependence ($1/v$ law) nearly identical to the dependence of the [35]Cl absorption cross section.

The only moderating material surrounding the detectors was 5 cm of light-weight polystyrene foam used to protect the equipment from impacts. Although this material and also the body and fuel tanks of the aircraft disturb the local "equilibrium" neutron flux, there should be very little systematic bias in the measured attenuation length if these factors are kept constant during the experiment. The fuel level is the only factor that would have changed over the course of the experiment. This effect was minimized by taking duplicate measurements with nearly full and nearly empty tanks.

On June 19, 2003, we conducted two series of flights from Keahole airport at Kailua-Kona, Hawaii (data given in Table 2 in the Appendix). In the first series, measurements were taken at 7 pressure altitudes from 500 m to 3800 m. After landing and refueling, another set of measurements was taken in the reverse order, beginning at 3800 m. To eliminate the possibility of a systematic bias due to decreasing fuel load during each flight, results from the two flights were averaged.

Pressure was logged at 1-min intervals from a sensor located in the unpressurized cabin of the airplane. Based on a comparison of GPS readings with open-cabin pressure logged during our flights in India, we estimate that open cabin pressures are correct to within 0.25%.

2.2.2. Neutron transport simulations

A premise of our low-energy neutron flux measurements is that at sufficient distance from the sea or ground surface the rate of production of fast neutrons and the rate of absorption of low-energy neutrons are in equilibrium. Near the interface of two materials having different neutron producing, moderating and absorbing properties, such as the air and water, this equilibrium is disturbed [16]. To ensure that our flight levels were in the equilibrium portion of the atmosphere, we calculated an altitude profile of low-energy neutron fluxes above seawater using the Monte Carlo N-Particle (MCNP) transport code, version 5 [17]. Our calculation assumes that the attenuation length for neutron production in both the atmosphere and seawater is 140 g cm^{-2}, and that neutron production is proportional to $A^{1/2}$ [18,19]. The neutron source is modeled with an evaporation energy spectrum with a 1 MeV peak and an isotropic angular distribution. Neutron fluxes were tallied in 20 energy bins from 0.001 to 150 eV. The detector response was simulated by weighting the fluxes in each energy bin by the average [3]He neutron absorption cross section for the energy bin and then summing the weighted fluxes over all bins.

The transport simulation indicates that the low-energy atmospheric neutron flux is in disequilibrium with neutron production in the region 1033–950 g cm^{-2} (0–680 m) (Fig. 3). The direction in which the flux is affected is a function of elevation above water, with fluxes 0–40 m above the surface being higher than the expected equilibrium flux and those from 40 to 680 m being lower. This suggests that neutron count rates recorded at 998 g cm^{-2} (300 m) and 962 g cm^{-2} (600 m) were disturbed by the air–water boundary and therefore should not be used to determine the attenuation length for the equilibrium portion of the atmosphere.
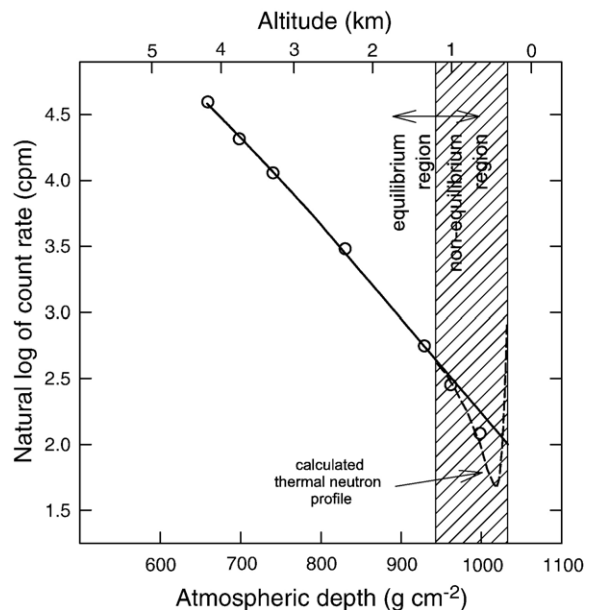

Fig. 3. Airborne measurements of low-energy neutron fluxes. The two measurements below 1000 m were affected by the presence of seawater, as indicated by our neutron transport simulations (dashed line).

2.3. Cutoff rigidities

The path of a primary cosmic-ray particle traveling through the geomagnetic field is controlled by the magnetic rigidity (momentum-to-charge ratio) of the particle. In order to reach a given location in the field, a particle must have a rigidity above the lower cutoff value for that location. All particles below the lower cutoff rigidity will be rejected by the field, but not all particles above the lower cutoff will be accepted. The energy above which all particles are accepted is defined as the upper cutoff rigidity. Between the lower and upper cutoffs particle trajectories are complex and there is often a fine structure of forbidden and accepted rigidity bands [20]. The effective cutoff rigidity, as defined below, takes into account the widths of these bands [20]. Because tropospheric nucleon fluxes are generated mostly in cascades initiated by primaries impinging at steep angles to the atmosphere, it is necessary to calculate effective cutoff rigidities only for vertically incident primaries [20].

In this work, we use effective vertical cutoff rigidity as a geomagnetic cutoff parameter. The purpose of a geomagnetic cutoff parameter is to uniquely order cosmic-ray data so that the primary cosmic-ray flux at a given cutoff value is always the same given the same galactic cosmic-ray flux. Effective vertical cutoff rigidity was calculated by numerically tracing the paths of primary cosmic-ray protons through International Geomagnetic Reference Field model 2000 [8,20]. The simulated trajectories correspond to vertically incident particles impinging on the atmosphere 20 km above each survey site. To obtain the effective vertical cutoff rigidity (R_C), we used the relation [21]:

$$R_C = R_U - \sum_{i=R_L}^{R_U} \Delta R_i \tag{2}$$

where R_U is the upper rigidity limit for forbidden trajectories, R_L is the lower limit for allowed trajectories and $\sum \Delta R_i$ is the sum of the allowed rigidity intervals between R_U and R_L.

The use of R_C to account for geomagnetic shielding represents an important advance in cosmogenic dating [4,5]. Parameters previously used to describe geomagnetic shielding effects were geomagnetic latitude calculated from a dipole model [22], geomagnetic latitude calculated from a high-order field approximation [23], surface values of geomagnetic inclination [24] and cutoff rigidity calculated from surface values of geomagnetic inclination and horizontal field intensity [25]. These previously used geomagnetic cutoff parameters do not have a unique relationship with cosmic-ray intensity and give discrepancies of up to ∼15% between fluxes at locations having the same parameter value, whereas discrepancies between fluxes at the same R_C are negligible.

3. Results and discussion

3.1. Energetic nucleons

3.1.1. Hawaii: comparison of neutron monitor responses

In order to verify that the response of the Arizona neutron monitor is similar to that of the more commonly used NM-64 neutron monitor, we compared our results from Mauna Kea, Hawaii to the NM-64 altitude survey conducted at Haleakala during the 1965 solar minimum [6]. The altitude dependence, as expressed by the effective attenuation length (Λ), was determined by fitting the equation:

$$\ln C = (1/\Lambda)x + b \tag{3}$$

to the count rates (C) by minimizing the chi-square merit function. Attenuation lengths obtained from Eq. (3) are termed *effective* because they assume that Λ is constant with x even though Λ is slightly altitude-dependent [6].

We obtained an effective attenuation length of 146.8±0.5 g cm^{-2} from our measurements over the depth range 1039.4–630.2 g cm^{-2} (0–4205 m), which is very close to the value of 146.8±0.2 g cm^{-2} obtained from [6]'s measurements over a similar range of altitudes (1033.9–725.0 g cm^{-2}, 0–3030 m) (Fig. 4). The agreement between the two surveys is very good considering that (1) the monitors have different designs, (2) [6]'s measurements are from solar minimum whereas ours are closer to solar maximum and (3) we covered a slightly greater elevation range. The good agreement with [6]'s data means that the Arizona neutron monitor can be used to extend their measurements, and therefore [5]'s scaling model which is based on those measurements, to R_C=17.3 GV.
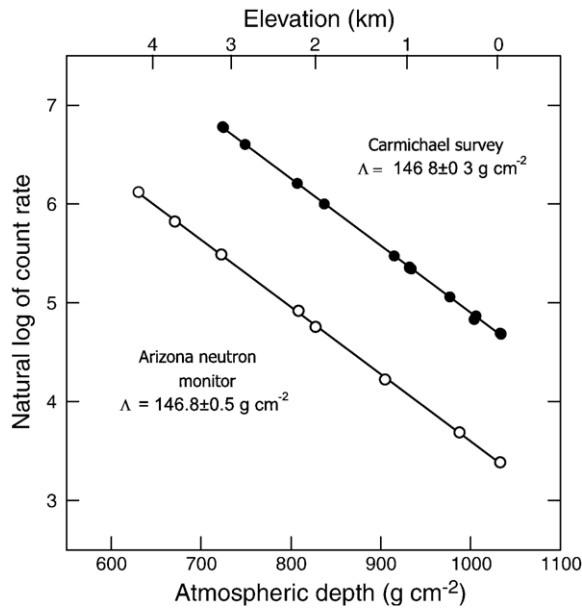
Fig. 4. Neutron monitor measurements of high-energy nucleon fluxes at Mauna Kea, HI in 2000 (this work) compared with measurements by Carmichael et al. [11] at Haleakala, HI in 1966. Counting rates from [11] are scaled down by a factor of 5000.

3.1.2. India: improved scaling parameters at low latitude

The attenuation length increases by only a small amount from Hawaii (R_C=12.8–13.3 GV) to India (R_C=17.3 GV) and this increase mostly is restricted to altitudes above 3000 m (Fig. 5). We obtained an effective attenuation length of 148.4 ± 1.3 g cm^{-2} at R_C=17.3 GV from ground-based measurements (1029.6–763.4 g cm^{-2}, 0–2637 m), which is very close to the values that we and [6] measured in ground-based surveys in Hawaii. At higher
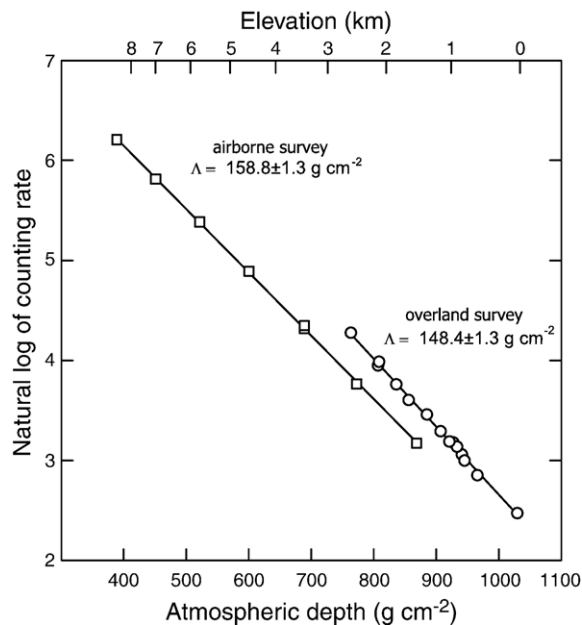

Fig. 5. Neutron monitor measurements from southern India, 2002. One detector was absent during the airborne survey, so count rates were lower than during the land-based survey.

Table 2
Coefficients for Eq. (4)

n	1.0177E−02
a	1.0207E−01
k	−3.9527E−01
a_0	8.5236E−06
a_1	−6.3670E−07
a_2	−7.0814E−09
a_3	−9.9182E−09
a_4	9.9250E−10
a_5	2.4925E−11
a_6	3.8615E−12
a_7	−4.8194E−13
a_8	−1.5371E−14

altitudes, our airborne measurements suggest a more substantial increase from the value of 153.5 ± 0.5 g cm^{-2} obtained from [6]'s transect at 13.3 GV and 724–367 g cm^{-2} (0–3030 m) to 158.8 ± 1.3 g cm^{-2} at 17.3 GV and 773 to 389 g cm^{-2} (2560–8250 m).

Based on the data from India, we give updated polynomial coefficients (Table 2) for scaling spallation reactions. The effective attenuation length for spallation reactions is well described by the formula:

$$\Lambda_{e,sp}(R_C, x_1, x_2) = \frac{x_2 - x_1}{\left[n(1 + \exp(-\alpha R_C^{-k}))^{-1}x + 1/2(a_0 + a_1 R_C + a_2 R_C^2)x^2 + 1/3(a_3 + a_4 R_C + a_5 R_C^2)x^3 + 1/4(a_6 + a_7 R_C + a_8 R_C^2)x^4 \right]_{x_1}^{x_2}} \tag{4}$$

where $\Lambda_{e,sp}$ is the effective attenuation length between x_1 and x_2. The new coefficients were determined by iteratively forcing Eq. (5) to agree with the muon-corrected effective attenuation lengths measured in India. This new parameterization is valid from $x = 1033$ g cm^{-2} to $x = 500$ g cm^{-2} (0–5700 m) and from $R_C = 0$ GV to $R_C = 17.3$ GV. Relative nucleon fluxes calculated over this altitude range from the parameters in Table 2 agree with our muon corrected data from India to within 2% on average, which is very good agreement considering that the uncertainty on individual measurements is ∼2% on average. Our earlier parameterization [5] matches our India data to within only 6%. We also refitted the high-latitude data in order to provide a better agreement with [6]'s results. The new high-latitude attenuation lengths are about 2% higher than before but are still within the +5/−2% uncertainty of the values given by [5]. The uncertainty in Λ propagates to a significant uncertainty in production rates if there is a large altitude range between the calibration site and sample site. For example, the uncertainty in scaling between 0 m and 5000 m (1033–540 g cm^{-2}) is +15/−17% at low latitude given a +5/−2% uncertainty in Λ.

3.1.3. How to applying scaling factors

For scaling cosmogenic nuclide production from a sea-level high-latitude (SLHL) calibration site ($x = 1033$ g cm^{-2}, $R_C < 2$) to a given x and R_C the scaling factor can be expressed as the product of separate latitude and altitude scaling factors:

$$F(R_C, x) = f(x)f(R_C) \tag{5}$$

where $f(R_C)$ is the latitude scaling factor at sea level, which is given by the Dorman function:

$$f(R_C) = 1 - \exp(-\alpha R_C^{-k}) \tag{6}$$

where $\alpha = 10.275$ and $k = 0.9615$ for spallation reactions [5,21]. The elevation scaling factor, $f(x)$, for spallation reactions is given by:

$$f(x) = \exp \frac{1033 - x}{\left[n(1 + \exp(-\alpha R_C^{-k}))^{-1}x + 1/2(a_0 + a_1 R_C + a_2 R_C^2)x^2 + 1/3(a_3 + a_4 R_C + a_5 R_C^2)x^3 + 1/4(a_6 + a_7 R_C + a_8 R_C^2)x^4 \right]_x^{1033}} \tag{7}$$

The production rate at a sample site $P(R_C,x)$ is then given by:

$$P(R_C, x) = P_0 \cdot F \tag{8}$$

where P_0 is the production rate at a SLHL calibration site. For scaling production rates between any two arbitrary locations (where neither is at SLHL), the scaling factor is given by the ratio of the scaling factors for each site relative to SLHL. For example, if a sea level low-latitude location has $F=0.5$ and a mid-latitude high-altitude location has $F=4$, then the production rate at the second site is eight times the rate at the first site.

3.2. Low-energy neutron fluxes

The apparent attenuation length determined from our airborne measurements of low-energy neutron fluxes is $\Lambda_{th}=149\pm4$ g cm^{-2} over the range 928–658 g cm^{-2} (950–3800 m). For the purpose of comparing with previous work [26], we also calculated Λ_{th} as a continuous function of depth by fitting a second-order polynomial

$$\ln C = b_1 x^2 + b_2 x + b_3 \tag{9}$$

to the natural logarithm of our count rates. A non-linear fit is justified by the observation that Λ_{th} changes rapidly with altitude [26], and therefore the use of an effective Λ over the entire altitude range may be inaccurate. The attenuation length is given by the derivative of Eq. (9):

$$1/\Lambda_{th}(x) = \frac{d\ln C}{dx} = 2b_1 x + b_2 \tag{10}$$

We performed a Monte Carlo simulation to determine the mean value and confidence limits for $\Lambda_{th}(x)$. For each data point, we generated 1000 synthetic data points randomly selected from a Gaussian distribution having the same mean value and standard deviation as the selected measurement. The mean and standard deviation of Λ_{th} was determined as a continuous function of x by fitting Eq. (9) to the simulated data sets and then applying Eq. (10).

The dependence of Λ_{th} on altitude that we determined is in excellent agreement with dependence found by [26] (Fig. 6). Both experiments suggest that low-energy neutron fluxes have a different altitude dependence than the more energetic component measured with a neutron monitor. The data on low-energy neutrons indicate that Λ_{th} is greater
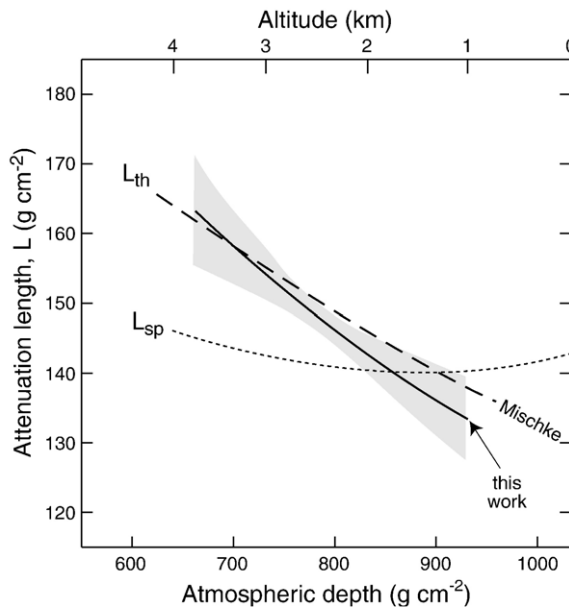

Fig. 6. Attenuation length for low-energy neutron fluxes as a continuous function of depth in the atmosphere from this work and from Mischke [26] at $R_C=12.8$ GV. The attenuation length for spallation reactions, Λ_{sp}, is shown for comparison.

than Λ_{sp} above 1500 m and that attenuation lengths for the two energy bands diverge with increasing altitude. This behavior is consistent with a nucleon energy spectrum that hardens with increasing altitude. However, in the lowermost 1500 m, [26]'s regression suggests that the relation between low- and high-energy neutron attenuation lengths is reversed. Our data do not have the precision to support or refute [26]'s results. We point out, however, that [26]'s regression includes measurements from closer to sea level ($x = 960$ g cm^{-2}) than our regression ($x = 929$ g cm^{-2}). The low-altitude measurements by [26] might have been taken in the non-equilibrium region near the air/water interface. According to our transport calculation (Section 2.2), measurements in the non-equilibrium region would produce a shorter Λ and hence could explain why attenuation lengths given by [26] are lower than expected below 1500 m.

4. Implications and considerations for surface exposure dating

4.1. Scaling production rates to higher paleomagnetic field strength

The anomalously high cutoff rigidity over India makes it possible to use modern cosmic-ray measurements to scale production rates to paleo-dipole fields that are greater in strength than the present dipole field (Fig. 7). This works because (1) the relation between cosmic-ray intensity and R_C is unique (to a good approximation [27]); (2) non-dipole components create locally higher (and lower) cutoff rigidities than would occur in a dipole field; (3) cosmogenic nuclide production is integrated over time; and (4) integrated paleomagnetic fields probably to a dipole over $\sim 10,000$ yrs [24,28,29]. The new measurements of nucleon fluxes at $R_C = 17.3$ GV are equivalent to measurements at the geomagnetic equator in a dipole field with a strength (M) ~ 1.2 times greater than the modern (1945) dipole strength of 8.084×10^{22} A m^2 (M_0). Our earlier parameterization [5] was valid at the equator up to $M/M_0 = 0.9$. At higher latitudes the parameterization is valid for greater field strengths because dipole strength fluctuations have only a small effect on cutoff rigidity toward the poles. For example, $M/M_0 = 1.4$ gives $R_C = 16.3$ GV at 25° geomagnetic latitude, which is within the range of our updated scaling parameterization.

The new parameterization covers nearly the full range of R_C values that have occurred at the timescale of surface exposure dating. Over the past 800,000 yr, dipole strength has remained between 0.3 and 1.4 times the current field strength [30]. Only over the past 10,000 yr has the dipole field been stronger than the modern field for a prolonged time [31]. The strongest paleomagnetic dipole fields (averaged over 500-yr intervals) exceeded $M/M_0 = 1.2$ for only ~ 3000 yr. That is important only to young samples from field sites near the geomagnetic equator, where the average R_C could have been as high as 20 GV from 1.5 to 3.5 ka. Extrapolation of our scaling model beyond $R_C = 17.2$ GV would be a potential source of error only for low-latitude samples with exposure ages on the order of a few thousand years.

4.2. Sensitivity of landform ages to energy-dependent scaling parameters

Do energy-dependent scaling factors make a difference in calculating landform ages? The answer to this question depends on the dominant nuclide production mechanisms in a sample (e.g. spallation versus thermal neutron activation) and on the location of the sample site relative to the calibration site. An extreme case would be in scaling a calibrated production rate from SLHL to a high-altitude (4000 m) equatorial ($R_C = 14.8$ GV) location. In this case, the scaling factor for low-energy neutron reactions would be 22% lower than for high-energy nucleons and ages would be $\sim 22\%$ higher using the low-energy scaling. Samples at high geomagnetic latitude and low elevation are less sensitive to the energy dependence of scaling parameterizations for two reasons. First, calibrated production rates are usually
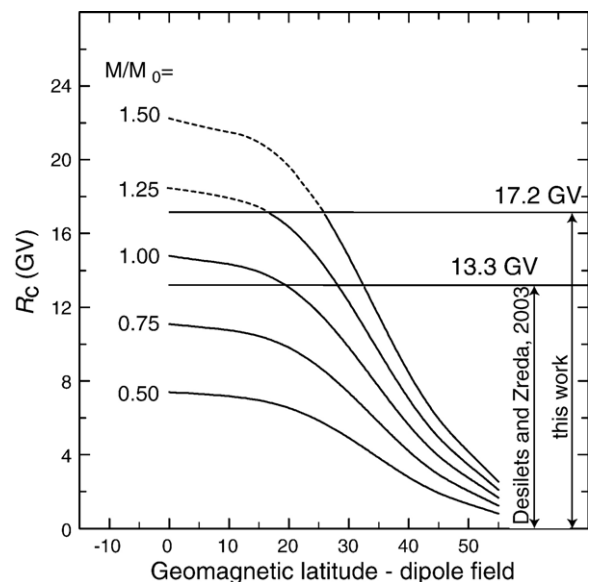

Fig. 7. Cutoff rigidity range of spallation scaling model for different dipole strengths.

normalized to high latitude and sea level, and therefore the scaling factor will be close to unity. Second, the two scaling models converge with increasing latitude and decreasing elevation.

4.3. Uncertainty in scaling factors

There are two categories of uncertainty associated with scaling factors. One category includes the fluctuating paleoenvironmental conditions that make determinations of x and R_C difficult for past epochs. Important paleoenvironmental variables include paleo-dipole position and strength (to which R_C is sensitive), and paleo-altitude and paleoclimate (to which x is sensitive). Solar modulation falls into this category because modulations of the galactic cosmic-ray flux have an effect similar to changes in R_C at high-latitude sites. Progress has been made in incorporating corrections for some paleoenvironmental effects (e.g. through use of paleomagnetic records) but corrections for paleo altitude, paleoclimate and solar activity are usually neglected. The magnitude of these commonly neglected corrections has not been fully evaluated.

The second type of uncertainty in scaling factors is related to errors in describing modern cosmic-ray fluxes. The spatial and temporal coverage of surveys, measurement errors and fitting errors contribute to the uncertainty of scaling models. As our work demonstrates, there is also a potentially large error in ignoring systematic differences between cosmic-ray measurements in the high- and low-energy bands. Another source of uncertainty is in the muon correction to the neutron monitor count rate, which mostly affects measurements at low altitude. More work is needed to quantify and minimize the errors in applying cosmic-ray measurements to cosmogenic nuclide scaling models.

It is impossible to make a uniform assessment of the error inherent in scaling production rates. There are a large number of potential errors and the sizes of these errors have spatial and temporal dependencies. For example, production rates will be most affected by solar activity near the poles and least affected near the equator, whereas the opposite is true for dipole strength variations. Furthermore, temporal fluctuations in production rates at a sample site may be correlated with similar changes at the calibration site and hence the errors at the two sites will cancel to produce a small error in the exposure age. In that case, corrections will only be valid if they are applied to both the calibration site and sample site; otherwise, landform ages could be overcorrected.

5. Conclusions

The measurements reported here extend the cutoff rigidity range of our spallation-reaction scaling model from 13.3 GV to 17.3 GV and provide new experimental evidence confirming that nucleon attenuation lengths depend on energy. The extended scaling model allows our scaling factors to be applied to higher paleomagnetic dipole strengths than were previously possible using other scaling formulations.

The major implication of energy-dependent attenuation lengths is that cosmogenic nuclides produced by different portions of the nucleon energy spectrum may require different scaling models. The scaling factor for neutron activation reactions may be smaller than that for spallation reactions by as much as 22%. The use of low-energy nucleon scaling factors is most relevant to ^{36}Cl dating, where both high- and low-energy production mechanisms can be important, and is more important for low-latitude samples, where the difference between Λ_{sp} and Λ_{th} is greatest.

Appendix A. Supplementary data

Supplementary data associated with this article can be found, in the online version, at doi:10.1016/j.epsl.2006.03.051.

References

[1] J.T. Fabryka-Martin, Production of radionuclides in the earth and their hydrogeologic significance, with emphasis on chlorine-36 and iodine-129, PhD dissertation, University of Arizona, 1988.
[2] D. Lal, B. Peters, Cosmic ray produced radioactivity on earth, in: K. Sitte (Ed.), Encyclopedia of Physics: Cosmic Rays II,

Encyclopedia of Physics, vol. 46/2, Springer-Verlag, Berlin, 1967, pp. 551–612.

[3] J.A. Simpson, W.C. Fagot, Properties of the low energy nucleonic component at large atmospheric depths, Phys. Rev. 90 (1953) 1068–1072.

[4] D. Desilets, M. Zreda, On scaling cosmogenic nuclide production rates for altitude and latitude using cosmic-ray measurements, Earth Planet. Sci. Lett. 193 (2001) 213–225.

[5] D. Desilets, M. Zreda, Spatial and temporal distribution of secondary cosmic-ray nucleon intensity and applications to in situ cosmogenic dating, Earth Planet. Sci. Lett. 206 (2003) 21–42.

[6] H. Carmichael, M. Bercovitch, V. Analysis of IQSY cosmic-ray survey measurements, Can. J. Phys. 47 (1969) 2073–2093.

[7] J.S. Pigati, N.A. Lifton, Geomagnetic effects on time-integrated cosmogenic nuclide production with emphasis on in situ ^{14}C and ^{10}Be, Earth Planet. Sci. Lett. 226 (2004) 193–205.

[8] M.A. Shea, D.F. Smart, A world grid of calculated cosmic ray vertical cutoff rigidities for 1980.0, Proceedings of the 18th International Cosmic Ray Conference MG 10-3, Bangalore, India, Tata Institute of Fundamental Research, Bombay, 1983, pp. 415–418.

[9] C.J. Hatton, The neutron monitor, in: J.G. Wilson, S.A. Wouthuysen (Eds.), Progress in Elementary Particle and Cosmic Ray Physics, vol. 10, North-Holland Publishing Co., Amsterdam, 1971, pp. 1–100.

[10] D.M. Desilets, The global distribution of secondary cosmic-ray intensity and applications to cosmogenic dating, M.S., University of Arizona, 2001.

[11] H. Carmichael, M.A. Shea, R.W. Peterson III, Cosmic-ray latitude survey in western USA and Hawaii in summer, 1966, Can. J. Phys. 47 (1969) 2057–2065.

[12] R. Pyle, P. Evenson, J.W. Bieber, J.M. Clem, J.E. Humble, M.L. Duldig, The use of ^{3}He tubes in a neutron monitor latitude survey, Proceedings of the 26th International Cosmic Ray Conference, vol. 7, Salt Lake City, AIP, Melville, N.Y., 1999, pp. 386–389.

[13] C.J. Hatton, H. Carmichael, Experimental investigation of the NM-64 neutron monitor, Can. J. Phys. 42 (1964) 2443–2472.

[14] G.F. Knoll, Radiation Detection and Measurement, Wiley, New York, 2000, 802 pp.

[15] Manual of the ICAO Standard Atmosphere extended to 80 kilometres (262 500 feet), International Civil Aviation Organisation, Doc. 7488, 1993.

[16] B. Liu, F.M. Phillips, J.T. Fabryka-Martin, M.M. Fowler, R.S. Biddle, Cosmogenic ^{36}Cl accumulation in unstable landforms: 1. Effects of the thermal neutron distribution, Water Resour. Res. 30 (11) (1994) 3115–3125.

[17] X-5 Monte Carlo Team, MCNP—A General Monte Carlo N-Transport Code, Version 5, Los Alamos National Laboratory, 2003.

[18] L. Dep, D. Elmore, J. Fabryka-Martin, J. Masarik, R.C. Reedy, Production rate systematics of in-situ produced cosmogenic nuclides in terrestrial rocks: Monte Carlo approach of investigating ^{35}Cl$(n,\gamma)^{36}$Cl, Nucl. Instrum. Methods Phys. Res., B 92 (1994) 321–325.

[19] S. Croft, L.C.A. Bourva, The specific total and coincidence cosmic-ray-induced neutron production rates in materials, Nucl. Instrum. Methods Phys. Res., A 505 (2003) 536–539.

[20] M.A. Shea, D.F. Smart, K.G. McCracken, A study of vertical cutoff rigidities using sixth degree simulations of the geomagnetic field, J. Geophys. Res. 70 (1965) 4117–4130.

[21] L.I. Dorman, G. Villoresi, N. Iucci, M. Parisi, M.I. Tyasto, O.A. Danilova, N.G. Ptitsyna, Cosmic ray survey to Antarctica and coupling functions for neutron component near solar minimum (1996–1997): 3. Geomagnetic effects and coupling functions, J. Geophys. Res. 105 (2000) 21,047–21,056.

[22] D. Lal, Cosmic ray labeling of erosion surfaces: in situ nuclide production rates and erosion models, Earth Planet. Sci. Lett. 104 (1991) 424–439.

[23] I.J. Graham, B.J. Barry, R.G. Ditchburn, N.E. Whitehead, Validation of cosmogenic nuclide production rate scaling factors through direct measurement, Nucl. Instrum. Methods Phys. Res., B 172 (2000) 802–805.

[24] T.J. Dunai, Scaling factors for production rates of in situ produced cosmogenic nuclides: a critical reevaluation, Earth Planet. Sci. Lett. 176 (2000) 157–169.

[25] T.J. Dunai, Influence of secular variation of the geomagnetic field on production rates of in situ produced cosmogenic nuclides, Earth Planet. Sci. Lett. 193 (2001) 197–212.

[26] C.F.W. Mischke, Intensiteisvaiasies van neutrone vanaf kosmiese strale, M.S., University of Potchefstroom (1972).

[27] J.M. Clem, J.W. Bieber, P. Evenson, D. Hall, J.E. Humble, M. Duldig, Contribution of obliquely incident particles to neutron monitor count rate, J. Geophys. Res. 102 (1997) 26,919–26,926.

[28] J.M. Licciardi, M.D. Kurz, P.U. Clark, E.J. Brook, Calibration of cosmogenic ^{3}He production rates from Holocene lava flows in Oregon, USA, and effects of the Earth's magnetic field, Earth Planet. Sci. Lett. 172 (1999) 261–271.

[29] T.M. Shanahan, M. Zreda, Chronology of Quaternary glaciations in East Africa, Earth Planet. Sci. Lett. 177 (2000) 23–42.

[30] Y. Guyodo, J.P. Valet, Global changes in intensity of the Earth's magnetic field during the past 800 kyr, Nature 399 (1999) 249–252.

[31] M.W. McElhinny, W.E. Senanayake, Variations in the geomagnetic dipole I: the past 50,000 years, J. Geomagn. Geoelectr. 34 (1982) 39–51.